END
DATE
FILMED
3 82
DTIC

1.0

4.5
5.0
5.6
6.2

2.8
3.2
3.6
4.0

2.5
2.2
2.0

1.1

1.8

1.25 1.4 1.6

MICROCOPY RESOLUTION TEST CHART
NATIONAL BUREAU OF STANDARDS-1963-A

REPORT DOCUMENTATION PAGE		READ INSTRUCTIONS BEFORE COMPLETING FORM
1. REPORT NUMBER Technical Report No. 2, 1981-82	2. GOVT ACCESSION NO. AD-A111 380	3. RECIPIENT'S CATALOG NUMBER
4. TITLE (and Subtitle) "Early Stages of Aging and Tempering of Iron-Carbon Martensites"		5. TYPE OF REPORT & PERIOD COVERED Technical; October 1981 - Sept. 1982
		6. PERFORMING ORG. REPORT NUMBER
7. AUTHOR(s) G. B. Olson and Morris Cohen		8. CONTRACT OR GRANT NUMBER(s) N00014-81-K-0013
9. PERFORMING ORGANIZATION NAME AND ADDRESS Massachusetts Institute of Technology Cambridge, MA 02139		10. PROGRAM ELEMENT, PROJECT, TASK AREA & WORK UNIT NUMBERS
11. CONTROLLING OFFICE NAME AND ADDRESS Office of Naval Research Arlington, VA 22217		12. REPORT DATE 1 February 1982
		13. NUMBER OF PAGES 29
14. MONITORING AGENCY NAME & ADDRESS(if different from Controlling Office)		15. SECURITY CLASS. (of this report)
		15a. DECLASSIFICATION/DOWNGRADING SCHEDULE

16. DISTRIBUTION STATEMENT (of this Report)

Unlimited

This document has been approved for public release and sale; its distribution is unlimited.

DTIC
ELECTE
FEB 2 5 1982

A

17. DISTRIBUTION STATEMENT (of the abstract entered in Block 20, if different from Report)

18. SUPPLEMENTARY NOTES

To be published in Metallurgical Transactions as part of the Peter G. Winchell Symposium on Tempering, held in Louisville, Kentucky, October 1981.

19. KEY WORDS (Continue on reverse side if necessary and identify by block number)

Aging and tempering of virgin martensites, structural changes and kinetics, carbon clustering and carbide precipitation.

20. ABSTRACT (Continue on reverse side if necessary and identify by block number)

The early stages of aging/tempering of iron-carbon martensites have been studied over a wide range of carbon contents by numerous experimental techniques. A kinetic framework is presented which allows a correlation of many diverse observations. Three general regimes of structural change termed relaxation, aging, and tempering can be further subdivided, thus identifying two stages of aging (A1 and A2) which precede the conventional stages of tempering (T1-T3). The first stage of aging involves clustering of carbon atoms in c-oriented octahedral sites, while the second stage is associated,

DD FORM 1473 1 JAN 73   EDITION OF 1 NOV 65 IS OBSOLETE
S/N 0102-014-6601

with a modulated tweed microstructure containing high-carbon regions which may be interpreted as either advanced carbon clusters or coherent transition carbides. Standard alloy compositions are proposed for further research to permit a more precise correlation of the diverse experimental observations required to interpret these unusual structures more completely.

Accession For

NTIS GRA&I

DTIC TAB

Unannounced

Justification

By

Distribution/

Availability Codes

Avail and/or

Dist   Special

A

DTIC

COPY

INSPECTED

2

EARLY STAGES OF AGING AND TEMPERING OF IRON-CARBON MARTENSITES*

G. B. Olson and Morris Cohen
Dept. of Mat. Sci. and Eng., M.I.T., Cambridge, MA

Abstract

The early stages of aging/tempering of iron-carbon martensites
have been studied over a wide range of carbon contents by numerous
experimental techniques. A kinetic framework is presented which allows
a correlation of many diverse observations. Three general regimes of
structural change termed relaxation, aging, and tempering can be further
subdivided, thus identifying two stages of aging (A1 and A2) which pre-
cede the conventional stages of tempering (T1-T3). The first stage of
aging involves clustering of carbon atoms in c-oriented octahedral
sites, while the second stage is associated with a modulated tweed
microstructure containing high-carbon regions which may be interpreted
as either advanced carbon clusters or coherent transition carbides.
Standard alloy compositions are proposed for further research to
permit a more precise correlation of the diverse experimental obser-
vations required to interpret these unusual structures more completely.

In April of 1980, an informal Tempering Seminar dealing especially with the early stages of aging and tempering was held at MIT. Unpublished MIT thesis research was re-examined in the light of recent x-ray diffraction data of Winchell and co-workers as well as the emerging atom-probe field-ion microscopy (FIM) studies at Oxford University. A wide range of alloy compositions (covering 0.1 to 2.0 w/o C) has been investigated by several experimental techniques, including electrical resistivity, transmission electron microscopy, and Mössbauer spectroscopy. Detectable stages of aging are found to occur in the vicinity of room temperature, but the correspondence among the diverse experimental findings has been unclear due to kinetic differences over the span of carbon contents investigated. We here present a tentative framework for the correlation of these observations, which evolved from the aforementioned informal Tempering Seminar. Professor P. G. Winchell participated actively in the discussions.

Electrical Resistivity

Of all the experimental techniques employed, electrical resistivity measurements have been carried out over the widest range of carbon contents and temperature-time conditions. Resistivity curves thus provide a useful guide for positioning various results within the sequences of structural changes which constitute the overall tempering process. In order to study the behavior of "virgin" martensites, resistivity measurements have been made on Fe-Ni-C alloys with sufficiently low M_s temperatures that carbon diffusion during the

martensitic transformation is essentially avoided.* As discussed by Sherman, Eldis, and Cohen[2], the general shape of the resistivity curves define three basic regimes of structural change. The earliest processes, which can occur at cryogenic temperatures, are attended by a slight decrease in resistivity ($\Delta\rho_I$). While there is x-ray diffraction evidence of some change in the tetragonality of the martensite in this regime[3], the resistivity behavior is likely dominated by a slight isothermal martensitic transformation of retained austenite under the conditions of testing. The processes taking place in this regime can be regarded as _relaxation_. When significant carbon diffusion can occur, beginning at approximately -40° C for convenient times, the resistivity rises, eventually passing through a peak ($\Delta\rho_{II}$). This regime has been termed _aging_. A later bend in such resistivity curves signifies the onset of the conventional first stage of _tempering_. The latter sets in at a fractional resistivity drop of about 40% of that accompanying the complete tempering process.

Kinetic analysis of the resistivity behavior gives an activation energy for the aging process appropriate for the diffusion of carbon in martensite. Consistent with the earlier results of Winchell and Cohen[4], the kinetics of this process are dependent on carbon concentration, proceeding more slowly with increasing carbon. However, the kinetics of the later well-known stages of tempering are found to correlate with an activation energy appropriate to dislocation-pipe diffusion of iron.

---

*The presence of nickel is believed to exert relatively little influence on the kinetics of aging and tempering; it increases the rate of cementite (θ-carbide) precipitation somewhat at higher temperatures.[1]

X-ray Diffraction

Some of the most precise structural information on the earliest stages of aging/tempering has come from the recent x-ray diffraction studies of Winchell and co-workers[1,5-9]. Using an elegant "pseudo-single crystal" diffractometer technique, reflections from specific martensite variants formed in an oriented austenite single crystal allowed independent study of the 200, 020, and 002 peaks during aging and tempering of initially-virgin martensites formed in situ. In addition to revealing that the symmetry of the martensite is actually orthorhombic rather than tetragonal[5] and elucidating the influence of austenitic condition on martensite symmetry[7], these investigations also (a) determined the iron-atom displacements around a carbon atom[9], (b) demonstrated full c-oriented octahedral-site occupancy in Fe-Ni-C virgin martensite[9], and (c) uncovered a number of surprising changes during the aging of virgin martensite[1,9].

The structural changes during the aging and tempering of Fe-18Ni-1.0C martensite observed by Chen and Winchell[1] can be summarized for present purposes by the behavior of the martensite 002 peak in Figure 2, denoting results for two crystals. Peak position (interplanar spacing), integrated intensity, and peak breadth are plotted vs. temperature for sequential isochronal treatments of the same specimens. With peak separation techniques[8], the behavior of three different peaks, labelled "M", "C", and "α", can be identified. The "M" peak corresponds to the original peak from the virgin martensite. The "C" peak is one previously attributed to "low-carbon martensite"[4,10], while the "α" peak represents the cubic matrix of martensite reached during the classical stages of tempering.

During the earliest period of aging (below room temperature), the
"M" peak is seen to maintain a fairly constant interplanar spacing
whereas its intensity diminishes. This is attributed by Chen and
Winchell[1,9] to a clustering of carbon atoms, which maintains a
constant mean iron-atom displacement while the mean-squared
displacement increases. Such clustering is consistent with previous
interpretation of the electrical-resistivity increase that accompanies
aging[11].

A striking result obtained during the first appearance of the
broad "C" peak is that comparison of the 002 interplanar spacings with
those of the 200 and 020 (the latter being similar to the α peak)
reveals a negative tetragonality ($c/a - 1 < 0$). In contrast to the
earlier interpretation that low positive tetragonality of this peak
arises from regions of reduced carbon content, Chen and Winchell have
concluded that the position of this peak is determined by severe
elastic distortion due to coherency strains in thin regions which
are nearly carbon-depleted. From the extreme initial breadth of
the "C" peak (Figure 2c), the regions were estimated to be about
30 Å in size[1].

Correlation of Observations: Normalized Diffusion Time

The relation of observations, such as those of Figure 2, to their
location on the resistivity curve of Figure 1 can provide a useful
guide for correlation with other experimental observations. The
corresponding resistivity data are not always available, but the
correspondence of the kinetics of resistivity change with diffusion
kinetics allows a convenient framework for estimating such
relationships.

A normalized diffusion time for a species of diffusivity D can be expressed as:

$$t' = \frac{4Dt}{\delta^2} \quad . \qquad \qquad [1]$$

Here, time is normalized to the time for a linear diffusion distance of one site spacing δ. The total linear diffusion distance is then $\sqrt{t'}$. This normalized diffusion time is also approximately equal to the number of diffusive jumps per diffusing atom. It can be regarded as a dimensionless time-temperature parameter for comparing the disparate aging/tempering data in the literature.

As suggested by Hillert[12], the composition-dependent diffusivity of carbon in martensite is estimated as:

$$D_C^{\alpha'} = (2 \times 10^{-6}) \exp[- \frac{84.1 + 14.0(\text{w/oC}) \frac{kJ}{mole}}{RT}] \frac{m^2}{sec} \quad . \quad [2]$$

This then defines a normalized diffusion time or time-temperature parameter for carbon, t_C', which in turn helps specify the "position" of any reported observation within the carbon-diffusion-controlled stages of aging. For the tempering stages governed by dislocation-pipe diffusion of iron, a normalized diffusion time, t_{Fe}', can be defined from the estimated dislocation-pipe diffusivity[13] of:

$$D_{Fe} = (3 \times 10^{-5}) \exp [- \frac{134 \frac{kJ}{mole}}{RT}] \frac{m^2}{sec} \qquad [3]$$

The relative resistivity curve for Fe-21Ni-0.4C[2] is shown in Figure 3 against the corresponding diffusion times t_C' and t_{Fe}' . The plotted points represent values after one hour at the temperatures indicated. The curve is drawn to reflect the general shape of available data[2] over a range of carbon contents (0.1 to 0.6 w/o).

Accordingly, the resistivity maximum can be roughly located at $t_c' = 80$ with the bend in the curve coming at $t_c' \approx 10^5$. The normalized time t_c' based on the Hillert relation for carbon diffusivity appears to reasonably represent the carbon dependence (over the range examined) of the aging kinetics up to the bend in the curve. Progress of the subsequent resistivity decrease during the classical tempering stages is more appropriately gauged by t_{Fe}'.

Focussing on the early carbon-diffusion-dependent stages, the x-ray diffraction data of Figure 2a are replotted in Figure 4 together with the estimated shape of the corresponding relative resistivity curve based on t_c'. Points on the resistivity curve are obtained from recent resistivity measurements[14] on an Fe-15Ni-1.0C alloy given identical sequential thermal treatments as in the Chen and Winchell experiments.[9] While the diffraction results indicate some overlap of the phenomena involved, the peak and bend of the resistivity curve are seen to bracket the portion of the aging regime dominated by the "C" diffraction peak. Thus, these characteristic features of the resistivity curve serve as convenient markers for defining various stages of the aging/tempering process.

The aging region between the peak and bend of the resistivity curve ($t_c' = 80$ to 10^5) is of special importance to the mechanical properties of Fe-C martensites. Hardness measurements at the liquid-nitrogen temperature for 0.2 to 0.8 w/o C by Winchell and Cohen (4) exhibit a hardness peak at $t_c' = 3 \times 10^3$, approximately the midpoint of this aging region. Similar measurements of the 0.6% offset compressive yield strength at the liquid-nitrogen temperature by Eldis and Cohen[15]

suggest a peak at t_c' closer to 10^5. By either measure, a significant strength increase of ~ 10 to 20% occurs during this portion of the aging regime. The indications of extreme internal stress at the beginning of this stage may also be of importance to mechanical behavior. In addition to the first appearance of the extremely broad "C" peak with elastic-distortion-induced negative tetragonality, Chen and Winchell[1] interpret a redistribution of the 200 and 020 diffraction-peak intensities beginning at $\sim 20°$ C as arising from internal plastic deformation via movement of martensitic twin boundaries. Plastic relaxations during tempering have been demonstrated before[16,17], but the Chen and Winchell finding represents the earliest (smallest t_c') detection in the aging/tempering process. The severe internal stresses driving this plastic flow may also play a significant role in the brittleness of nominally "untempered" martensite. A metallographic study of microcracking in Fe-15Ni-1.0C[18] revealed that virgin martensite polished at the liquid-nitrogen temperature contains very few microcracks, but appreciable microcracking accompanies subsequent aging at room temperature when conditions corresponding to the resistivity peak are approached.

Two basic models have been proposed for the microstructure underlying the stage of aging associated with the appearance of the "C" diffraction peak. One interpretation[2] is an advanced stage of carbon clustering (in c-oriented octahedral sites of the martensite) for which carbon-deficient regions become sufficien y large ' diffract separately. On the other hand, Chen and Winchell[1] have proposed that elastically-

distorted carbon-depleted regions responsible for the "C" peak arise from the actual precipitation of a coherent form of a transition carbide which later adopts its less coherent form during the conventional first stage of tempering. The essential difference between these models lies in the structure of the carbon-rich regions which the available x-ray diffraction information does not directly reveal.

Mössbauer Spectroscopy

Clues to the structure of the high-carbon regions can be sought from available Mössbauer spectra, sensitive to the local bonding environment of iron atoms, as obtained from splat-quenched Fe-1.86 w/o C[19,20]. Analysis of the virgin-martensite spectra identifies three basic types of iron sites consistent with carbon occupancy of octahedral interstitial sites; retained austenite spectra suggest nonrandom occupancy of austenite interstitial sites at this high carbon content, suggestive of a repulsive carbon-carbon interaction in austenite. Development of the martensite spectra during room-temperature aging has been interpreted in terms of carbon clustering. New spectra appearing indicate two additional types of iron sites with a population ratio of 1:3 and a ratio of hyperfine magnetic fields of 3:2. From the similarity of these features to those of the two sites in the Fe_4N structure, an isomorphous Fe_4C structure has been proposed[19] as a reasonable model for the "clustered state." This corresponds to an ordered array of carbon atoms in c-oriented octahedral sites. Although these two types of sites are well-defined, the breadth of the spectral peaks suggests a distribution of compositions deviating from exact Fe_4C stoichiometry. Long aging at 80° C eventually produces a new spectrum identified as ε-carbide.[19]

Locating this structural information on the time/temperature resistivity curve could potentially resolve the issue of whether the structure present after the resistivity peak is an advanced stage of clustering or whether it represents precipitation of a coherent transition carbide. Unfortunately, extrapolation of the Hillert relation (Equation 2) to this high carbon content gives a carbon-diffusion activation energy considerably larger than that deduced experimentally from the changes in Mössbauer spectra on aging.[20] The larger value would suggest that the Mössbauer aging (clustering) observations were conducted entirely before the resistivity peak, whereas the smaller value would place them entirely after the peak. This situation is further confounded by preliminary resistivity measurements[14,21] which indicate that the resistivity peak is absent during the aging of very high-carbon martensites.

Transmission Electron Microscopy

Similar kinetic uncertainties becloud the assimilation of observations by high-resolution electron microscopy as obtained on very high-carbon martensites[22-24]. However, microscopy has been performed over a sufficiently wide range of carbon contents that findings on lower-carbon alloys,[2,22] for which precise kinetic data are available, can provide a key to correlating the observations at hand. A characteristic "tweed" microstructure is found to be associated with the portion of the aging regime bounded by the peak and bend of the resistivity curve in Figure 4. Examples of such structures are shown in Figure 5. Fine-scale features in high-carbon martensites vary from $\sim$10 Å wavelength modulations on $(102)_M$ with 102 satellite reflections, as reported by Nagakura[23] (Figure 5b), to $\sim$100 Å

modulations on $(011)_M$ as observed by Sachdev and Vander Sande[22] (Figure 5a) in conjunction with still finer features on $(102)_M$. A similar tweed pattern noted just after the resistivity peak in an Fe-21Ni-0.4C alloy[21] is shown in Figure 5c. As reported by Sherman et al.[2], such tweed features apparently persist until the bend in the resistivity curve.

The above microstructures are very similar to tweed structures attributed to arrays of elastically interacting particles acting as tetragonal strain centers in anisotropic BCC alloys[25]. From detailed analysis of images and diffraction effects, Nagakura et al.[23,24] have concluded that this type of microstructure is produced by $(102)_M$ modulations in the density of small ($\sim$10 Å) carbon clusters with approximately one-half the c-oriented octahedral sites occupied in these high-carbon clusters. Ordering of the carbon atoms in the Nagakura cluster model according to the Fe_4C structure may account for the two iron sites indicated by the Mössbauer spectra; this possibility is now being investigated[14].

Further aging leads to a number of interesting microstructures[22-24] which might be interpreted as coherent forms of ε or η carbide,* but so far the only unambiguous identification of transition carbides by electron diffraction occurs well into the conventional first stage of tempering, i.e., beyond the bend in the resistivity curve[2].

Atom-Probe Microanalysis

Further information that potentially can allow a distinction

---

* In some cases, the transition carbide traditionally described as HCP ε carbide is determined by electron diffraction to possess an ordered arrangement of carbon atoms accompanied by a slight ortho-rhombic distortion of the unit cell.[26,27] The designation η has been proposed for this ordered form of transition carbide having an Fe_2C structure isomorphous with Co_2C[26].

between carbon clusters and coherent carbides has been sought from
fine-scale chemical analysis provided by atom-probe field-ion
microscopy (AP/FIM), and this has been recently applied to the aging
and tempering of virgin martensites by Miller and Smith[28,29].
Results for 0.4C Fe-Ni-C martensites transformed and aged in situ
are summarized in Figure 6. The average compositions of high-carbon
regions, which tend to image darkly in the FIM, are designated by.
the square points together with bars denoting the range of values
observed in these regions. The average compositions of the lower-
carbon "matrix" regions are designated by the round points, with bars
again representing the range of values observed. Results from the
various time-temperature conditions examined are plotted vs. t_c'
in Figure 6.

Surprisingly, some evidence is obtained for carbon clustering in
the as-quenched virgin martensite. The matrix carbon concentration is
found to be slightly below the ~2 a/o (~0.4 w/o) carbon content of the alloy
(indicated by C_o in Figure 6), and high-carbon regions are detected with
concentrations as high as 7.8 a/o C (1.6 w/o). However, it is not yet
clear to what extent this clustering might be an artifact due to carbon
migration on the specimen surface prior to field-evaporation for the
measurements.

Aging at room temperature evidently enhances the observed clustering,
as reflected in a decrease in matrix carbon concentration along with
an increase in the high-carbon regions. Within the limits of spatial
resolution and analytical statistical requirements of the technique
employed, there is no evidence of Fe_4C regions in the clustered state

of this alloy. From the observed ratio of cluster composition to the overall carbon content, however, cluster compositions near Fe_4C seem plausible for the ~9 a/o C (~1.9 w/o C) alloy upon which the Mössbauer spectroscopy and Fe_4C cluster model are based[19].

The earliest clear indication of carbide precipitation in Figure 6 occurs after 24 hr. at 40° C. A high-carbon region approaching the $Fe_{2.4}C$ ε-carbide composition is detected with an associated drop in the minimum matrix carbon concentration. A discrepancy exists in that these effects are not noted after one hour at 100° C, corresponding to a higher value of t_c'. Nevertheless, after 24 hours at 100° C similar evidence for carbide precipitation is obtained. There is no finding to suggest carbide carbon concentrations as high as Fe_2C. Tempering 1 hour at 250° C indicates precipitation of Fe_3C θ-carbide with depletion of the matrix carbon to a negligible level.

Stages of Aging: Questions Remaining

The correspondences of observations (on the basis of the t_c' parameter) by x-ray diffraction, electrical resistivity, transmission electron microscopy, and atom-probe microanalysis, are summarized in Figure 7. Analogous to the conventional stages of tempering which can be designated T1, T2, and T3, etc., the diffraction and resistivity measurements suggest that the aging regime identified in Figure 1 can be subdivided into at least two stages of aging, designated as A1 and A2 in Figure 7. As discussed earlier, the peak and bend of the resistivity curve, at $t_c' \approx 80$ and $t_c' \approx 10^5$, provide convenient markers for the "boundaries" of these stages, although some overlapping of the phenomena at play is to be expected.

According to the bulk of the evidence pointed out thus far, the process underlying stage A1 is the clustering of carbon atoms occupying c-oriented octahedral sites in the martensite. Stage A2 is characterized by the appearance of the "C" diffraction peak (Figure 7a) attributed to low-carbon regions sufficiently coarsened to diffract separately, and a modulated tweed microstructure (Figure 7c) attributed to the elastic interaction of high-carbon regions acting as centers of tetragonal distortion. The nature of these high-carbon strain centers has been variously proposed as advanced carbon clusters[2,23] or coherent transition carbides[1]. Although the first carbides are only unambiguously identified (by electron microscopy) well into the conventional first stage of tempering (Figure 7c) and detailed analysis of the tweed microstructure supports the cluster model, the atom-probe compositional evidence for transition-carbide precipitation during stage A2 (Figure 7d) still leaves open the possibility that the Chen and Winchell coherent-carbide proposal may be valid.

While the normalized diffusion parameters can reasonably define time/temperature locations on the resistivity curve, and the latter in turn provides a convenient framework for correlation of existing experimental information, discrepancies such as those encountered in the atom-probe observations (e.g. 40C, 24 hr. vs. 100 C, 1h) demonstrate that this correlation should be regarded only as approximate. Due to thermodynamic differences with varying temperature (or carbon content), the same point on the resistivity curve, when arrived at by different time-temperature paths, does not necessarily correspond to the same microstructure. Discussion at the informal 1980 Tempering Seminar identified the need for some standard alloy compositions so that future experiments on aging and tempering may direct the diverse techniques toward clearer

interpretations of the key structures developed under conditions of identical composition, temperature, and time. The compositions proposed are given in Table I. It was unanimously agreed at the Seminar that a 1.0C alloy will provide an excellent standard due to the available Chen and Winchell precision x-ray diffraction information for this carbon content[1]. Use of one-hour treatments at the temperatures employed by Chen and Winchell likewise offers a standard series of aging/tempering conditions with precise diffraction information as a sound basis for comparison among the several techniques. An 0.4C alloy given the same treatments will furnish another convenient standard due to the relatively large amount of information already available for this carbon level as well as its close relation to the composition of commercial martensitic steels. The proposed nickel contents are designed to give an M_s temperature of -40° C in polycrystalline form, thereby allowing easy formation of virgin martensites. Further work on compositions near 2.0C for which the Mössbauer spectroscopy and high-resolution TEM observations are available is also desirable, but difficulties of specimen preparation and higher M_s temperatures (which cannot be easily lowered by nickel additions due to graphitization problems) render these less convenient as standard alloys for a wider range of experimental techniques.

The microstructure associated with the A2 stage of aging offers a most interesting area for future research. The aging kinetics of the Fe-15Ni-1.0C standard alloy are sufficiently slow to allow practical examination of the evolution of microstructural features through this entire regime beginning at the resistivity peak. The fine scale of the tweed structure presents a challenge to developing high-resolution

microscopy techniques. Judging from $(101)_M$ lattice-fringe images of the $(102)_M$ modulated structure[23,24], it appears that plane-by-plane atom-probe microanalysis at a $(101)_M$ pole may provide the ultimate resolution of the precise compositions of the uncertain high-carbon strain centers underlying this unusual microstructure. An understanding of this structure and its evolution may also allow better control of the mechanical behavior of "untempered" martensite.

Conclusions

A normalized diffusion parameter has provided a framework for the correlation of available diverse experimental findings on the early stages of aging and tempering of Fe-C martensites over a wide range of carbon contents. Regimes of structural change termed relaxation, aging, and tempering can be further subdivided, identifying two stages of aging which precede the conventional stages of tempering. The first stage corresponds to clustering of carbon atoms in c-oriented octahedral sites. The second stage involves a fine modulated tweed microstructure containing elastically distorted carbon-deficient regions which are sufficiently coarse to yield a separable x-ray diffraction peak. Associated high-carbon regions have been attributed either to an advanced stage of clustering or to coherent transition carbides.

Standard alloy compositions are proposed to allow a more precise understanding of aging/tempering phenomena in iron-carbon martensites. Particular attention should be directed in this context to the unusual tweed-like microstructure which sets the stage for the processes of classical tempering and which controls the mechanical behavior of "untempered" martensite.

Acknowledgments

The informal 1980 Tempering Seminar at MIT from which this paper
evolved was catalyzed by the stimulating contributions of Peter Winchell
who, during his all-too-brief career, provided the _life force_ that
pervaded research on the tempering of martensite over the past two
decades.

Very helpful discussions were also contributed by Drs. N. DeCristofaro
(Allied Corporation), G. T. Eldis (Climax Molybdenum), M. K. Miller
(U. S. Steel Corporation), A. K. Sachdev (General Motors Corporation),
A. M. Sherman (Ford Motor Company), G. D. W. Smith (Oxford University),
and J. B. Vander Sande (MIT). Resistivity measurements crucial to the
correlations obtained in this paper were performed by K. A. Taylor
(MIT).

References

1. P. C. Chen and P. G. Winchell: _Met. Trans. A_, 1980, vol. 11A,
   pp 1333-39.

2. A. M. Sherman, G. T. Eldis, and M. Cohen: This volume.

3. M. Hayakawa, Y. Uemura, and M. Oka: _Met. Trans. A_, 1981, vol. 12A,
   pp 1545-47.

4. P. G. Winchell and M. Cohen: _Trans. ASM_, 1962, vol. 55, pp 347-61.

5. A. K. Sachdev and P. G. Winchell: Met. Trans. A, 1975, vol. 6A, pp 59-63.

6. V. G. Veeraraghavan and P. G. Winchell: Met. Trans. A, 1975, vol. 6A, pp 701-05.

7. M. M. Hall and P. G. Winchell: Acta Met., 1977, vol. 25, pp 735-50.

8. M. M. Hall, V. G. Veeraraghavan, H. R. Rubin, and P. G. Winchell: J. Appl. Crystallogr., 1977, vol. 10, pp 66-68.

9. P. C. Chen, B. O. Hall, and P. G. Winchell: Met. Trans. A, 1980, vol. 11A, pp 1323-32.

10. L. I. Lysak, Ya. N. Vouk, A. G. Drachinskaya, and Yu. M. Polishchuk: Phys. Met. Metallogr., 1967, vol. 24, pp 95-100.

11. D. W. Hoffman and M. Cohen: Acta Met., 1973, vol. 21, pp 1215-23.

12. M. Hillert: Acta Met., 1959, vol. 7, p. 653-58.

13. N. A. Gjostein: Diffusion, pp 241-74, ASM, 1973.

14. K. A. Taylor: MIT doctoral research in progress.

15. G. T. Eldis and M. Cohen: This volume.

16. R. L. Brown, H. J. Rack, and M. Cohen: Mat. Sci. Eng., 1975, vol. 21, pp 25-34.

17. T. A. Balliett and G. Krauss: Met. Trans A, 1976, vol. 7A, pp 81-86.

18. T. Vilo and J. Pietikäinen, Proc. Int. Conf. Mart. Transf. (ICOMAT-79), pp 721-27, MIT (Cambridge, MA), 1979.

19. W. K. Choo and R. Kaplow: Acta Met., 1973, vol. 21, pp. 725-32.

20. N. DeCristofaro, R. Kaplow, and W. S. Owen: Met. Trans. A, 1978, vol. 9A, pp 821-25.

21. A. K. Sachdev: Sc.D. Thesis, MIT, June 1977.

22. A. K. Sachdev and J. B. Vander Sande: This volume.

23. S. Nagakura, Y. Horotsu, M. Kusunoki, T. Suzuki, and Y. Nakamura: This volume.

24. M. Kusunoki and S. Nagakura: J. Appl. Crystallogr., 1981, vol. 14, pp 329-36.

25. P. J. Fillingham, H. J. Leamy, and L. E. Tanner: Electron Microscopy and Structure of Materials, ed. G. Thomas, Univ. Cal. Press (Berkeley) 1972).

26. Y. Hirotsu and S. Nagakura: Acta Met., 1972, vol. 20, pp. 645-55.

27. D. L. Williamson, K. Nakazawa, and G. Krauss: Met. Trans. A, 1979, vol. 10A, pp 1351-63.

28. M. K. Miller, P. A. Beaven, G. D. W. Smith, and S. S. Brenner: Proc. Int. Conf. Solid-Solid Phase Transf., Carnegie-Mellon Univ., AIME, 1982.

29. M. K. Miller, P. A. Beaven, S. S. Brenner, and G. D. W. Smith: This volume.

Figure Captions

Table I. Standard Tempering Alloy Compositions (w/o)

Fe-15Ni-1.0C

Fe-25Ni-0.4C
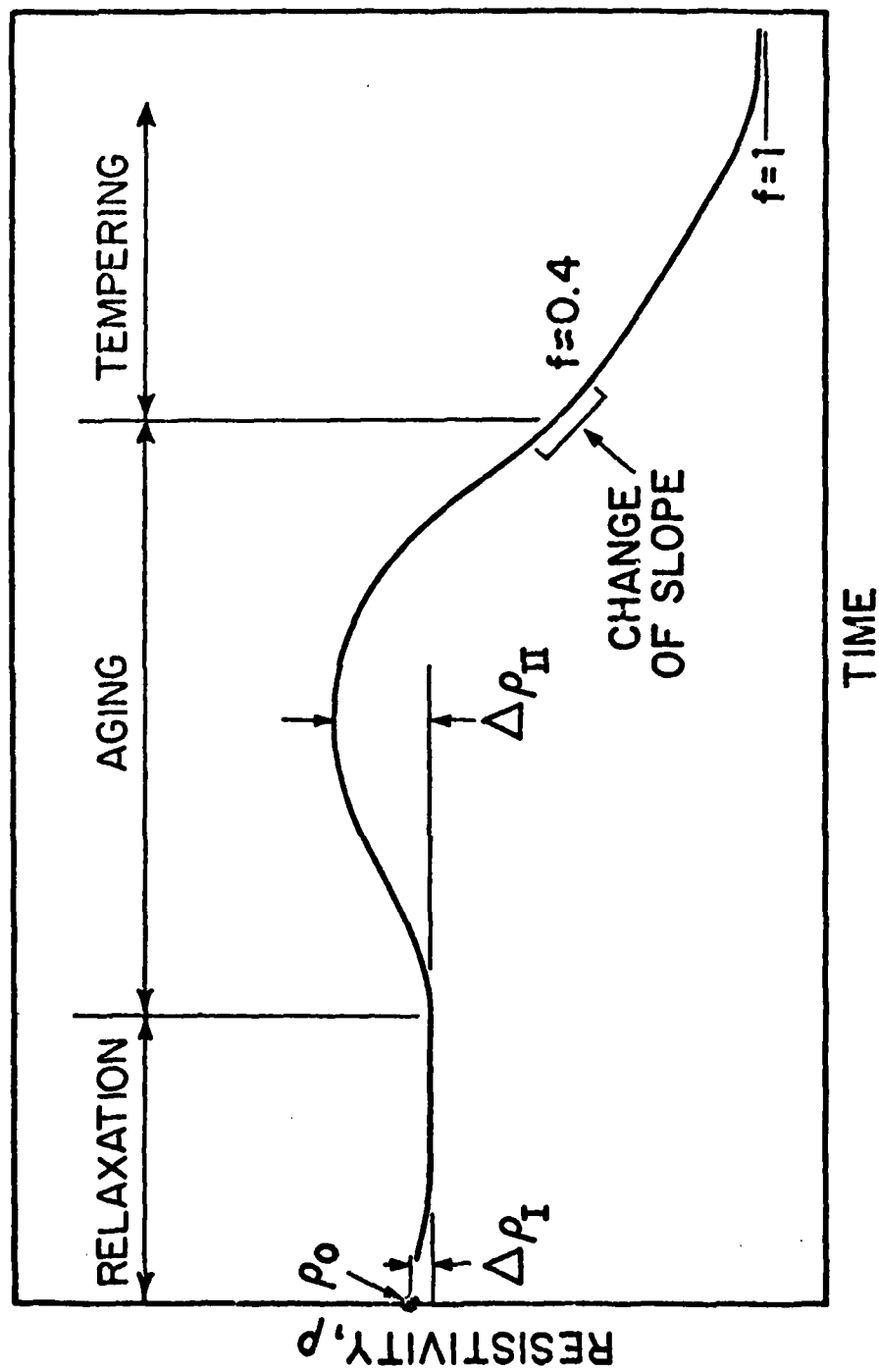
Figure 1
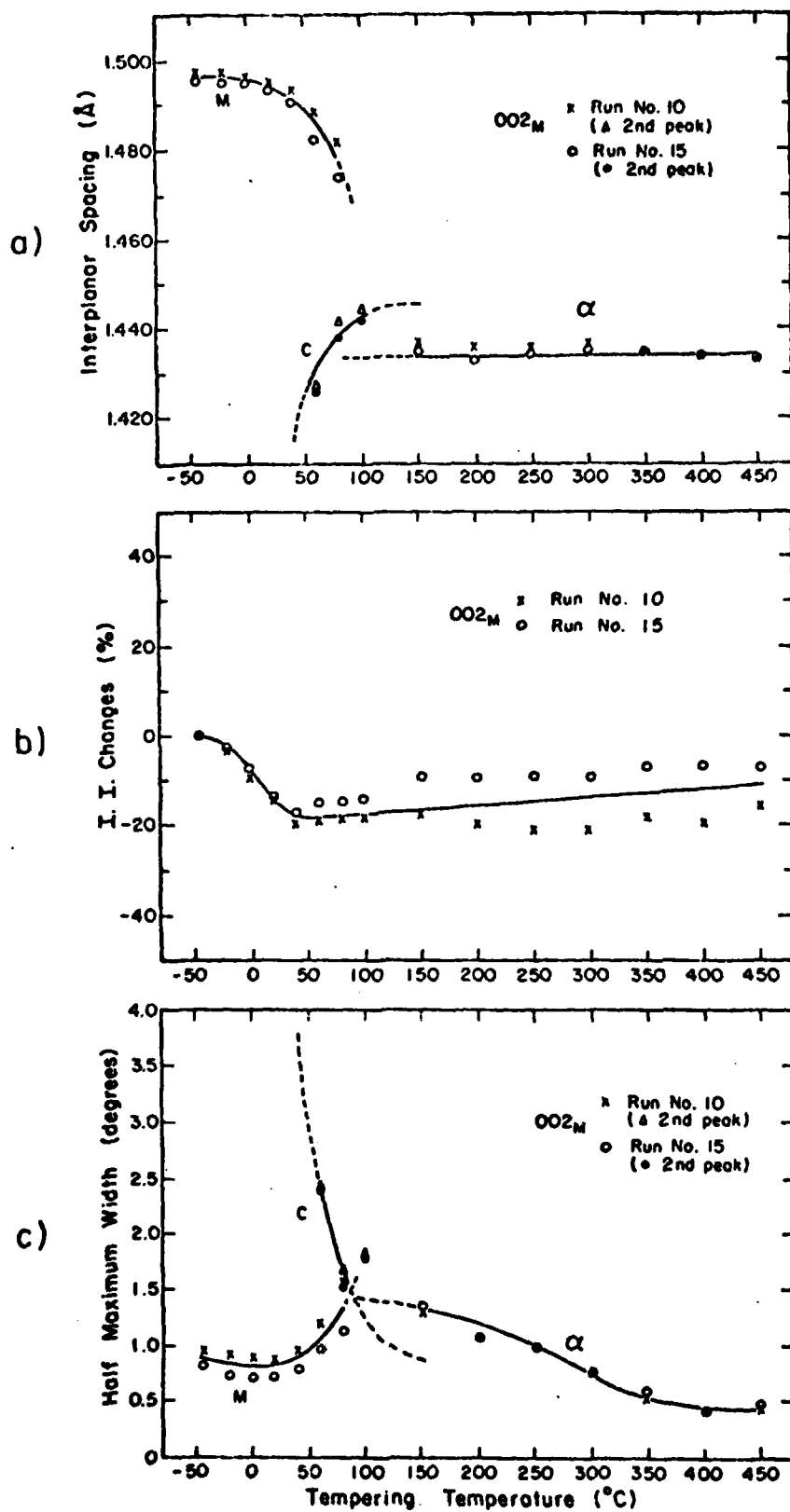
Figure 2
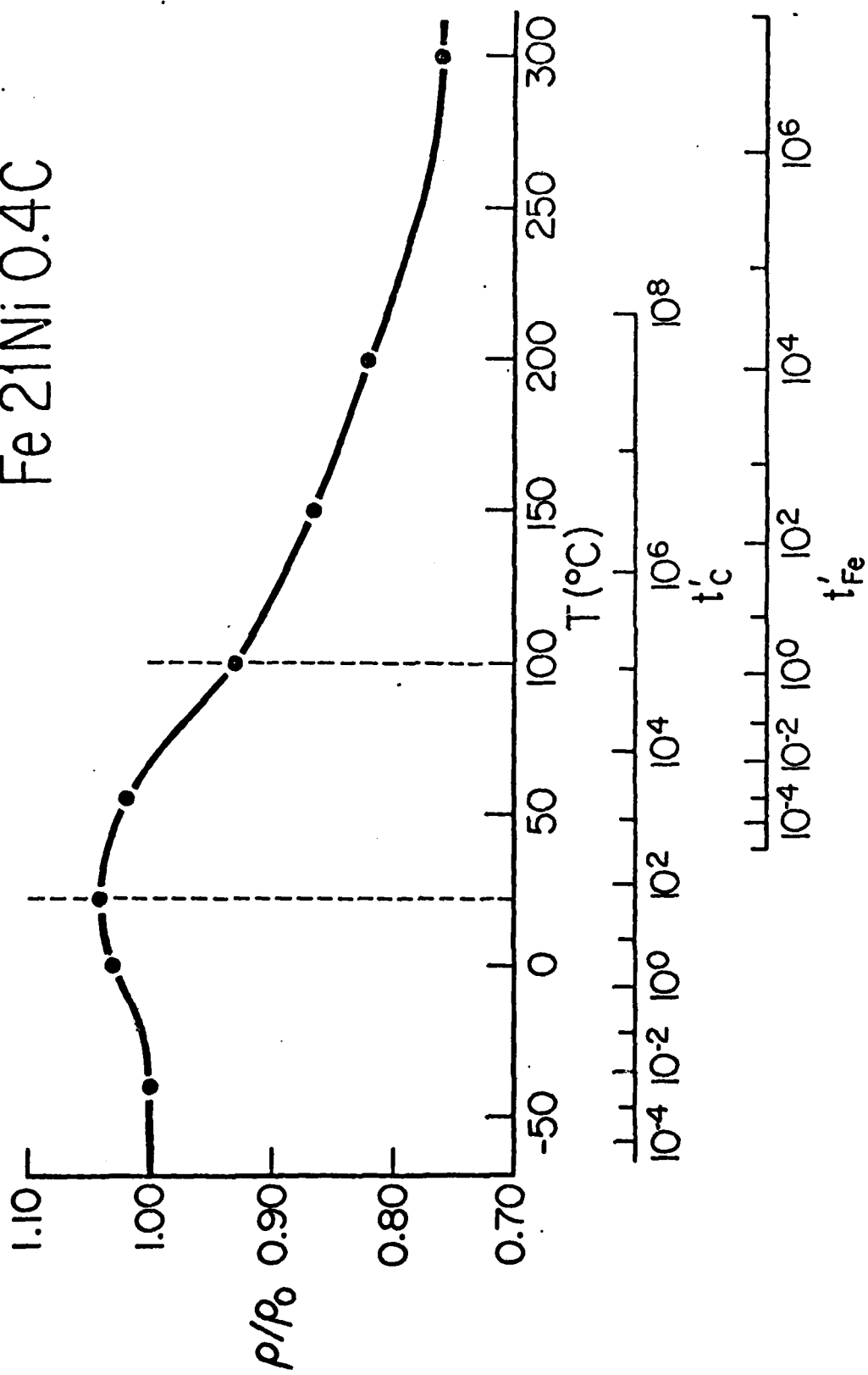
Figure 3

Figure 4

a)

b)

c)

Figure 5

Figure 6

Fe 23-29Ni 0.4C

Axis labels: a/o C (vertical), t'_c (horizontal)

Reference lines: Fe_2C, $Fe_{2.4}C$, Fe_3C, Fe_4C, C_0

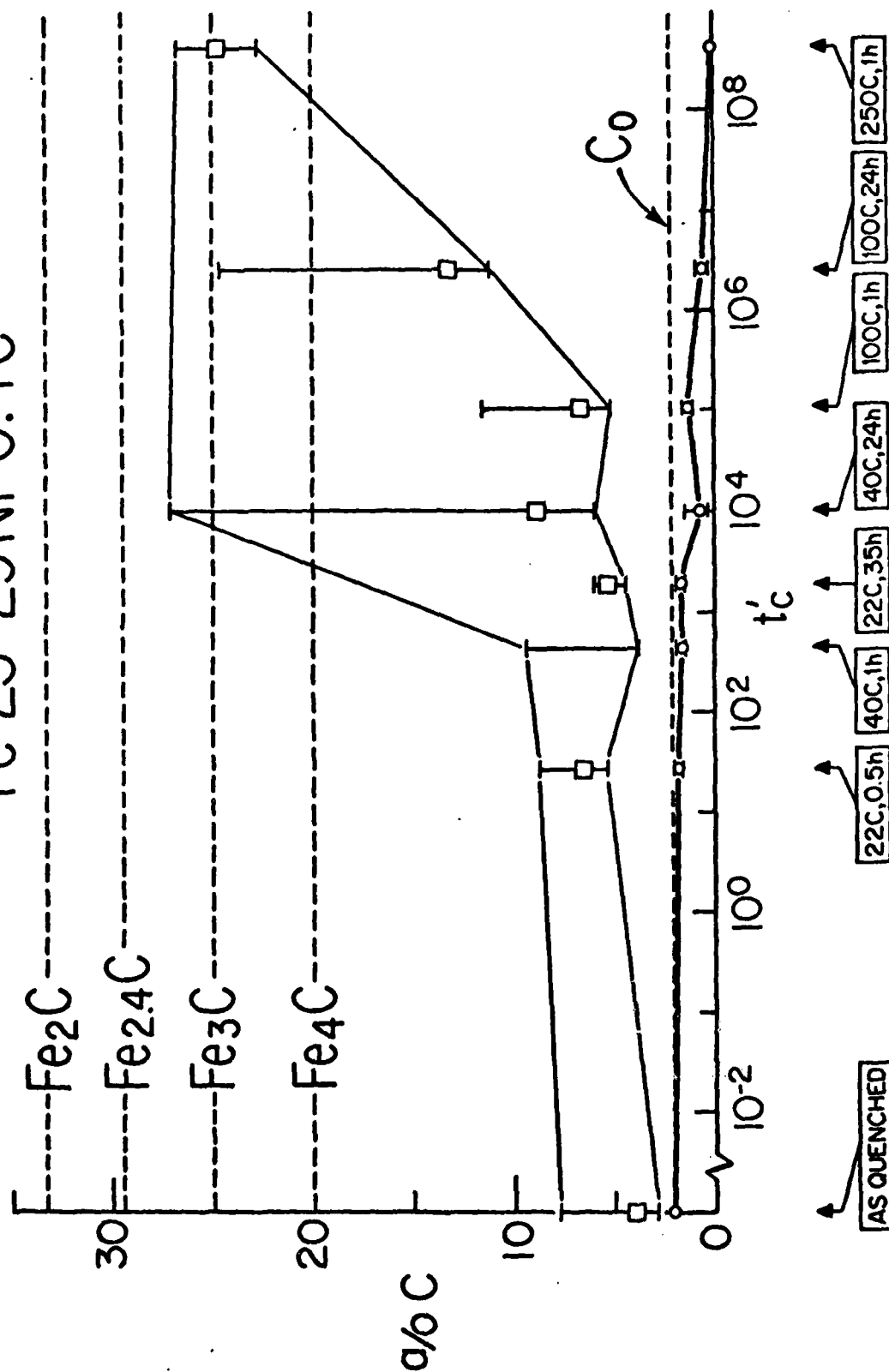Legend arrows: AS QUENCHED, 22C,0.5h, 40C,1h, 22C,35h, 40C,24h, 100C,1h, 100C,24h, 250C,1h
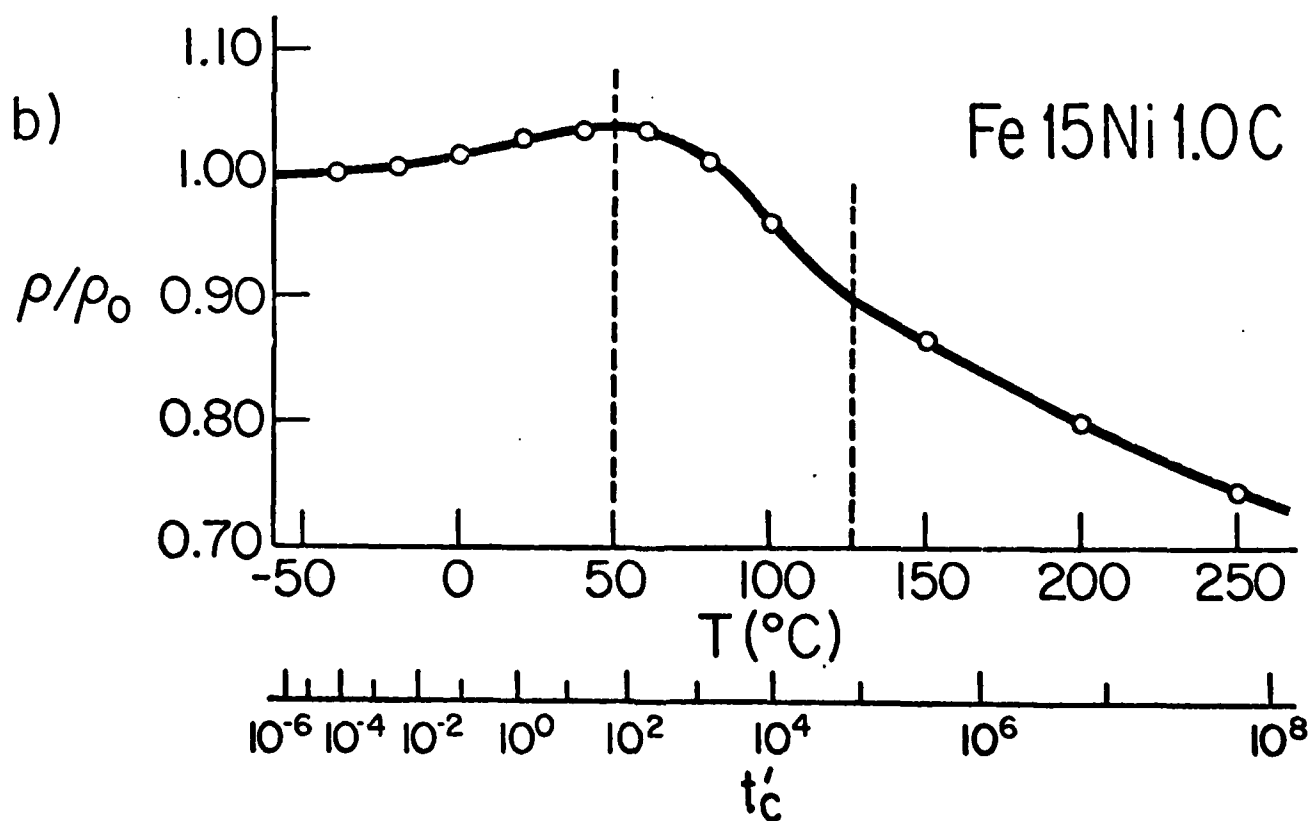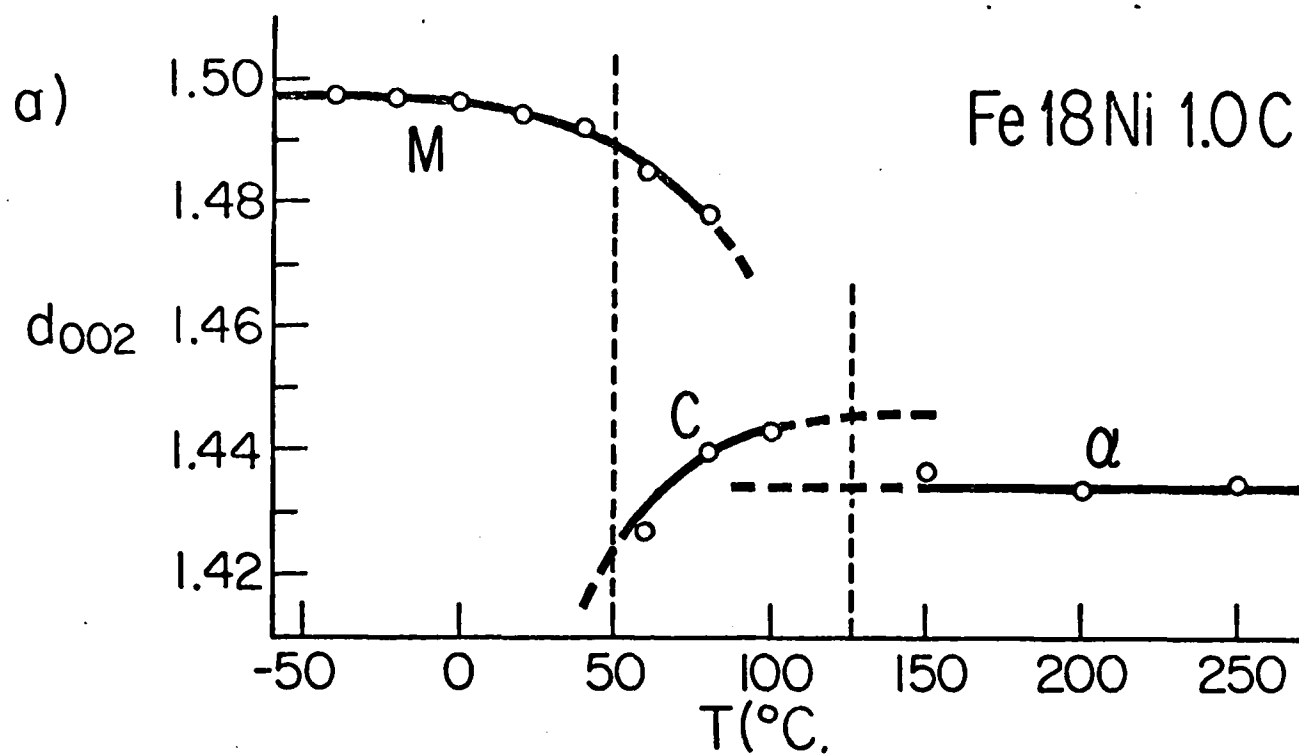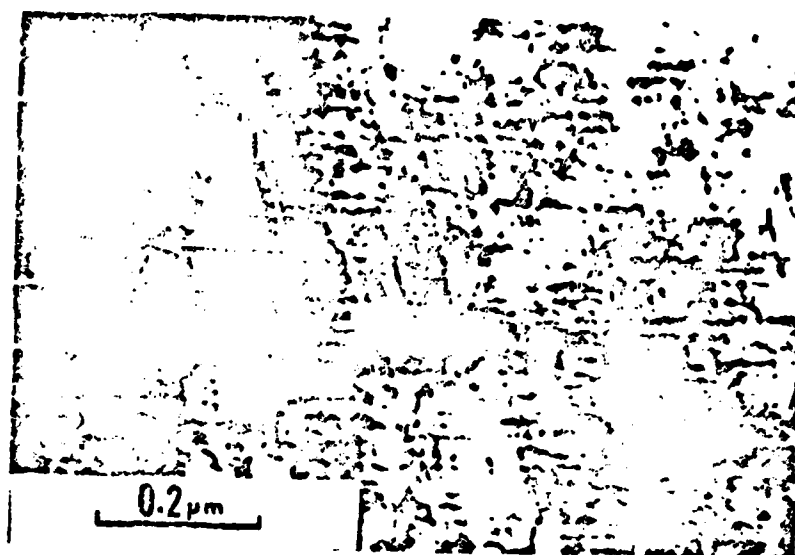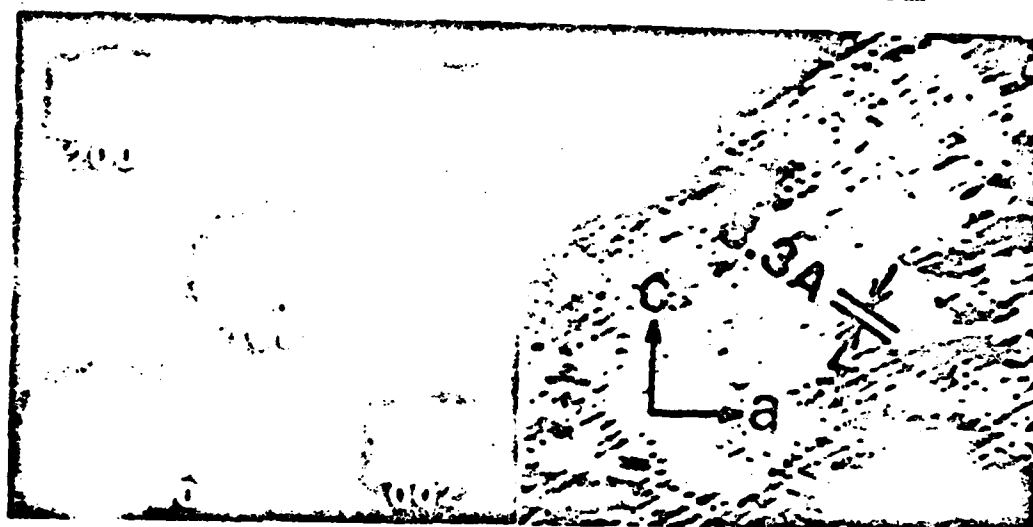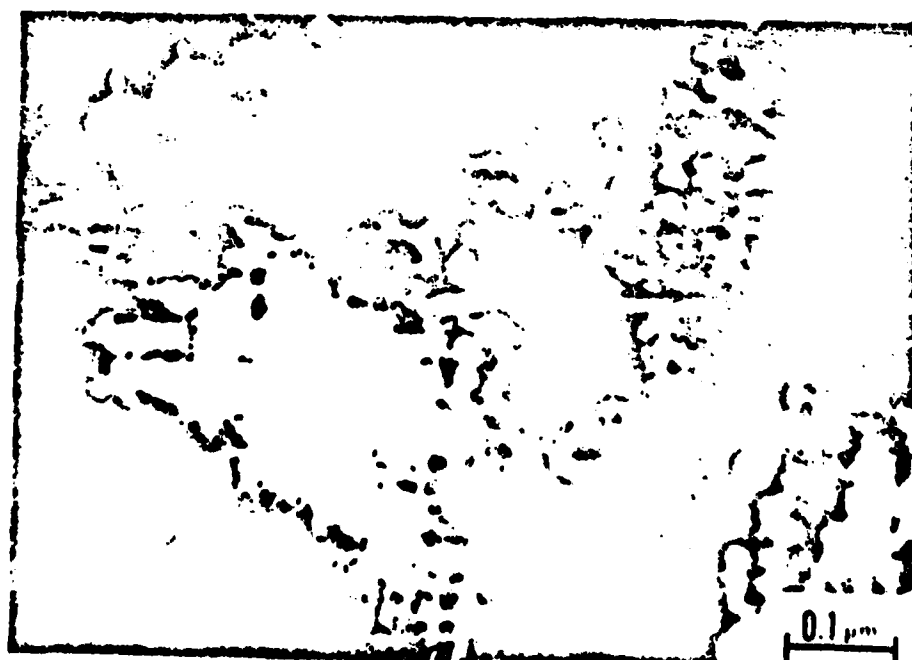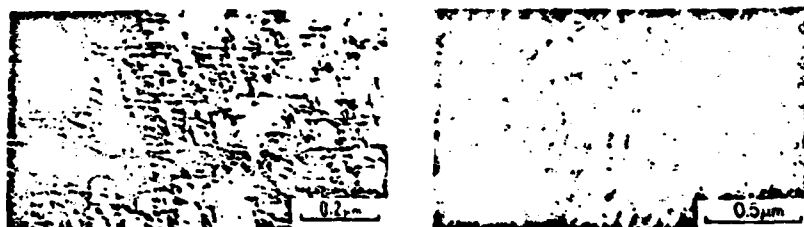
a) X-ray diffraction
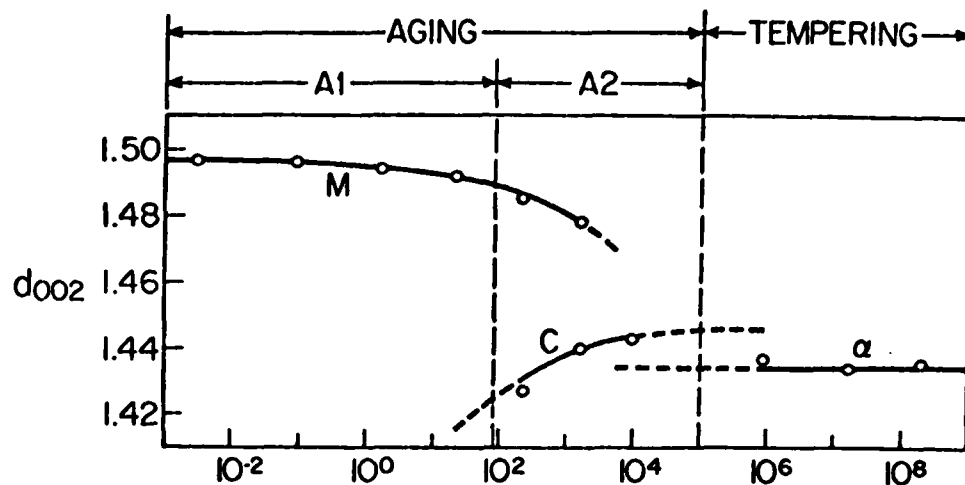
b) Electrical resistivity
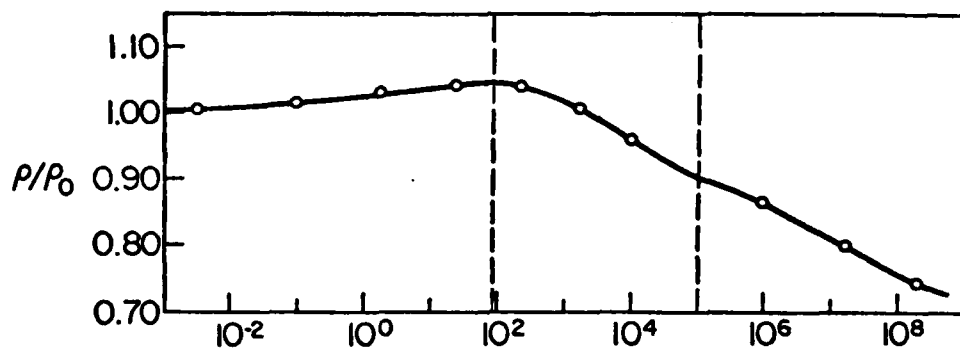
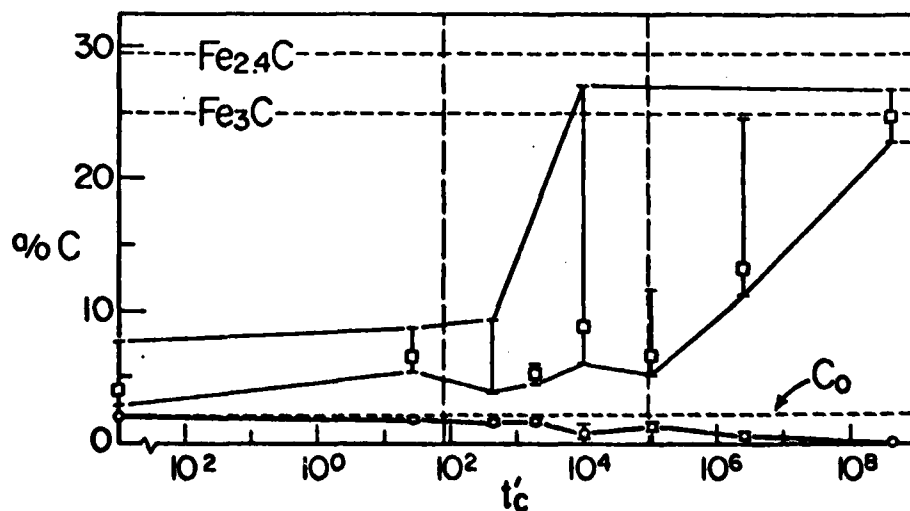c) Transmission electron microscopy

d) Atom-probe microanalysis

Figure 7

END

DATE
FILMED

3-82

DTIC